

Subtraction method in the second random-phase approximation: first applications with a Skyrme energy functional

D. Gambacurta,¹ M. Grasso,² and J. Engel³

¹*Dipartimento di Fisica e Astronomia and INFN, Via Santa Sofia 64, I-95123, Catania, Italy*

²*Institut de Physique Nucléaire, IN2P3-CNRS, Université Paris-Sud, F-91406 Orsay Cedex, France*

³*Department of Physics and Astronomy, University of North Carolina, Chapel Hill, North Carolina 27516-3255, USA*

We make use of a subtraction procedure, introduced to overcome double-counting problems in beyond-mean-field theories, in the second random-phase-approximation (SRPA) for the first time. This procedure guarantees the stability of SRPA (so that all excitation energies are real). We show that the method fits perfectly into nuclear density-functional theory. We illustrate applications to the monopole and quadrupole response and to low-lying 0^+ and 2^+ states in the nucleus ^{16}O . We show that the subtraction procedure leads to: (i) results that are weakly cutoff dependent; (ii) a considerable reduction of the SRPA downwards shift with respect to the random-phase approximation (RPA) spectra (systematically found in all previous applications). This implementation of the SRPA model will allow a reliable analysis of the effects of 2 particle-2 hole configurations ($2p2h$) on the excitation spectra of medium-mass and heavy nuclei.

PACS numbers: 21.60.Jz, 21.10.Re

I. INTRODUCTION

Energy-density functional (EDF) theories have evolved over the years with the formulation and application of sophisticated methods that go beyond mean-field theory. One example is the SRPA model, formulated long ago [1, 2] but applied in full only very recently because of the extreme numerical effort required. The last few years have seen large-scale SRPA calculations done without approximations in the matrices and with high-energy cutoffs [3–8]. Performing such calculations has allowed us to identify some specific features of the SRPA model, that could not be seen in previous strongly truncated and simplified calculations. Unexpectedly, the SRPA spectrum is systematically lowered by several MeV with respect to that obtained in the ordinary RPA. The origin of this strong shift was unclear until recently.

One would think that the SRPA, which adds $2p2h$ states to the 1 particle-1 hole ($1p1h$) states of the RPA, should not greatly modify excitations in which $1p1h$ configurations represent the dominant contribution. The improvements provided by the SRPA should be the following: 1) For cases in which the $1p1h$ states are the most important configurations and the RPA properly describes the location of the main peaks of the response function, the SRPA should not change those locations much. In addition, the coupling to $2p2h$ states should provide some spreading and improve the calculated widths, which in the RPA are far too small. 2) For cases in which multiparticle-multipole configurations are essential to describe the excitation, the SRPA model should yield not only spreading widths, but also a substantially different description of the overall strength distribution than does the RPA. Only recently it has started to become clear that the unexpected shift in SRPA energies is intimately related to the implicit inclusion of correlations in ground states; properly accounting for those correla-

tions would guarantee a stable ground state and thus a consistent response function.

In Refs. [5–8], SRPA calculations were performed with density-dependent effective interactions — the Skyrme [9–11] and the Gogny [12, 13] interactions — that derive from EDFs and are used extensively in medium-mass and heavy nuclei. Kohn-Sham-based density-functional theory (see next section) requires that EDF parameters be adjusted through mean-field calculations to reproduce properties of nuclear matter as well as masses and radii of some selected nuclei. However, mean-field calculations, even with density-dependent interactions, fail to reproduce several aspects of nuclear phenomena. Higher-order corrections (and correlations) may be explicitly introduced by going beyond the mean-field approximation. One must then depart from strict density-functional theory and treat the interaction as an explicit Hamiltonian. Such beyond-mean-field calculations may lead to several problems associated with mixing EDFs (which generate effective interactions with non-antisymmetric matrix elements) and genuine Hamiltonian many-body theory. Moreover, when higher-order corrections are explicitly introduced, the parameters of the interaction should be readjusted to avoid problems of double counting [14]. In the particular framework of extended RPA theories, such as SRPA, this would imply that different interactions are used for the description of the ground state and of excited states, with a lack of self-consistency leading to possible admixing of spurious states in the physical spectrum.

Some years ago [15], Tselyaev proposed another procedure to avoid double-counting, called the “subtraction” method. It has been applied thus far mainly to models that include particle-vibration coupling, specifically both the non-relativistic [16–18] and relativistic [19–21] versions of the time-blocking approximation. More recently [22], Tselyaev formally demonstrated that this procedure guarantees the validity of the usual stability condition in extensions of the RPA. The stability of the RPA is re-

lated to the Thouless theorem [23], which states that the Slater determinant on which the RPA is based must be a minimum of the Hartree–Fock (HF) energy to guarantee real RPA eigenvalues. Ref. [22] showed that this theorem does not hold in general for extended versions of the RPA, such as the SRPA, and that the subtraction procedure reinstates it.

For the SRPA with a real density–independent Hamiltonian, the problem of stability was addressed in a different way by Papakonstantinou [24]. The author showed that: (i) the Thouless theorem can be extended to the SRPA model if an explicitly correlated ground state is used; (ii) in spite of the stability problem, the energy–weighted sum rule (EWSR) [23, 25] is satisfied within the SRPA model, confirming a previous study by Yannouleas [2]. Indeed, an extension of SRPA with a correlated ground state was applied to metallic clusters in the work reported in Ref. [26]. The standard SRPA with a HF ground state produced a significant shift of strength towards lower energies with respect to the RPA strength function. The use of a correlated ground state, however, pushed the strength back towards larger energies, closer to the RPA (and experimental) results. In this kind of calculation, the shift is clearly due to a consistent ground state, of which an account of correlations and stability are both clearly important features.

As already mentioned, however, explicit correlations (for example, a correlated ground state in SRPA) may be problematic in an EDF–based calculation. The ground state of an EDF–based model already has an energy and density designed to be as close as possible to the exact ones. The Tselyaev subtraction procedure, by contrast, fits beautifully into density functional theory, as we show in the next section, and is much less costly numerically. It has in addition the great advantage of simultaneously removing double–counting problems and instabilities. This is the procedure adopted in the present work.

In subsequent sections, we apply the subtraction procedure within the SRPA for the first time, to the monopole and the quadrupole giant resonances of the nucleus ^{16}O , as well as to its low–lying 0^+ and 2^+ states. We will compare the results with those of the ordinary RPA and with experiment. We perform the calculations with the Skyrme functional SGII [27], both in the mean–field equations and in the effective residual interaction. We omit Coulomb and spin–orbit contributions in the residual interaction but include rearrangement terms following Ref. [6].

The article is organized as follows: Section II discusses the subtraction method in the context of density–functional theory. Section III presents our formalism and discusses a convenient “diagonal” approximation. Section IV illustrates the results obtained with the subtracted SRPA, and assesses the accuracy of the diagonal approximation. Section V compares subtracted SRPA response functions with those of the ordinary RPA and with experiment. Section VI presents conclusions.

II. SUBTRACTION METHOD AND DENSITY–FUNCTIONAL THEORY

It is difficult to say exactly what is meant by a density–dependent interaction, particularly when it does not have antisymmetric two–body matrix elements. In practice such an interaction is always used to construct an expression for the energy, which is then varied to obtain mean–field equations. It turns out to be natural not to worry about the interaction and to work instead with the energy as a functional of various densities — the ordinary number density, the spin–density, etc. The condensed–matter and atomic–physics communities have seized on this idea, the elaboration of which is known as density functional theory [28].

The foundation of the theory consists of the Hohenberg–Kohn theorem [29] and the Kohn–Sham procedure [30]. These building blocks have to be modified slightly for nuclear physics so that they work with densities that are defined with respect to the nuclear center of mass, but they survive the modification intact [31]. To simplify matters here, we pretend that only the intrinsic one–body density $\rho(\mathbf{r})$ is relevant; that is, we neglect other densities and currents on which the functional typically depends. Density functional theory then works with the object $E[\rho]$, the meaning of which is the smallest expectation value of the underlying nuclear Hamiltonian produced by states that yield density ρ . Thus, one finds the system’s ground–state energy and density by minimizing $E[\rho]$. The Hohenberg–Kohn theorem states that the energy–density functional $E[\rho]$ is universal: in the presence of an additional local operator $\lambda Q(\mathbf{r})$, with λ an arbitrary constant, $E[\rho]$ is modified in a simple way,

$$E[\rho] \longrightarrow E_\lambda[\rho] = E[\rho] + \lambda \int d\mathbf{r} Q(\mathbf{r})\rho(\mathbf{r}). \quad (1)$$

The Kohn–Sham procedure guarantees that any energy–density functional can be written in terms of orbitals $\varphi_i(\mathbf{r})$, as if the system consisted of noninteracting particles in a density–dependent external potential, and that the ground state energy and density can be found by solving the Hartree–like equations for the orbitals that come from minimizing the functional with respect to the orbital wave functions. Skyrme and Gogny energy–density functionals for a given nucleus make perfect sense when interpreted as approximations to the Kohn–Sham functional.

Now suppose that the multiplier λ is small. Then, system’s density changes from the unperturbed ground–state density ρ_0 to a new one ρ_λ , given by

$$\rho_\lambda = \rho_0 + \lambda \int d\mathbf{r} R(\omega = 0, \mathbf{r}, \mathbf{r}')Q(\mathbf{r}), \quad (2)$$

where $R(\omega = 0)$ is the static response function for the underlying Hamiltonian. Because the energy functional is universal, it reproduces ρ_λ exactly when modified as in Eq. 1. And in the Kohn–Sham approach, the functional produces a mean–field effective Hamiltonian (that

nonetheless reproduces exact energies and densities), so that the response function $R(\omega = 0)$ is given by the RPA, which is the small-amplitude limit of time-dependent mean-field theory [25]. In other words

$$R(\omega = 0) = R_{KS}^{RPA}, \quad (3)$$

where R_{KS}^{RPA} is the RPA response associated with the Kohn–Sham representation of the functional and the corresponding ground-state Slater determinant. Thus, to the extent that the Skyrme functional is the exact Kohn–Sham functional, Skyrme–RPA produces the exact zero-frequency response function, and any modification of the response must vanish in the static limit. This is what is meant by “avoiding double counting,” a fact that was noted by Tselyaev in Ref. [22].

More generally, one can show through a time-dependent version of the Hohenberg–Kohn theorem (known as the Runge–Gross theorem [32]) and a time-dependent Kohn–Sham procedure that the full response function at any frequency obeys

$$R(\omega, \mathbf{r}, \mathbf{r}') = R_{KS}^0(\omega, \mathbf{r}, \mathbf{r}') + \int d\mathbf{r}_1 d\mathbf{r}_2 R_{KS}^0(\omega, \mathbf{r}, \mathbf{r}_1) V(\omega, \mathbf{r}_1, \mathbf{r}_2) R(\omega, \mathbf{r}_2, \mathbf{r}'), \quad (4)$$

where R_{KS}^0 is the bare Kohn–Sham (mean-field) response and $V(\omega)$ is a frequency-dependent effective interaction obtained from the time-dependent energy-density functional $\mathcal{E}[\rho(t), t]$. The approximation

$$V(\omega, \mathbf{r}_1, \mathbf{r}_2) \longrightarrow \frac{\delta^2 E[\rho]}{\delta\rho(\mathbf{r}_1)\delta\rho(\mathbf{r}_2)} \Big|_{\rho_0} \equiv V^{RPA}(\mathbf{r}_1, \mathbf{r}_2), \quad (5)$$

implies that the solution R is just R_{KS}^{RPA} , which does not depend on ω . The approximation is equivalent to assuming that $\mathcal{E}[\rho(t), t] = E[\rho(t)]$, that is, that the time-dependent energy is just the ground-state functional evaluated at the time-dependent density. Making that approximation is known as the adiabatic limit. To go beyond that limit, one must introduce an ω dependence into the effective two-body interaction V . That, as we will see shortly, is precisely what the SRPA does. But since R_{KS}^{RPA} is correct (as correct as the Skyrme functional, anyway) in the adiabatic limit, we must modify the SRPA so that it gives the RPA response at $\omega = 0$.

There are many ways one might modify the SRPA $V(\omega)$ so as to obtain the RPA response in the adiabatic limit. One could, for example, simply multiply $V^{SRPA}(\omega)$ by a function that is unity at large ω and falls to $V^{RPA}/V^{SRPA}(0)$ as ω goes to zero. But the response function has other constraints as well; in particular the

quantity $\text{Im}[\int d\mathbf{r} d\mathbf{r}' Q(\mathbf{r}) R(\omega, \mathbf{r}, \mathbf{r}') Q(\mathbf{r}')] must have real and positive residues at poles on the positive real axis, that is, it must produce a genuine strength function (the stability condition). Although there may be more than one way to ensure this, a particularly simple way is the subtraction method. If we define the frequency/energy-dependent difference between the SRPA and RPA effective interactions by $U(\omega)$,$

$$U(\omega) \equiv V^{SRPA}(\omega) - V^{RPA}(\omega), \quad (6)$$

the subtraction procedure amounts to the replacement

$$V^{SRPA}(\omega) \longrightarrow V^{SRPA}(\omega) - U(0), \quad (7)$$

which guarantees, as required, that $V^{SRPA}(0) = V^{RPA}(0)$ after the substitution and thus that this “subtracted SRPA” reduces to the RPA in the zero-frequency limit.

In the next section we describe how the method works in the matrix version of the SRPA.

III. SUBTRACTION METHOD IN SRPA

Here we work with the matrix formulation of the SRPA. Details about the associated formalism appear, for instance, in Ref. [2]. Details about the subtraction method and its specific application to extended RPA models can be found in Refs. [15, 22].

The SRPA equations can be written in the following form:

$$\begin{pmatrix} \mathcal{A} & \mathcal{B} \\ -\mathcal{B}^* & -\mathcal{A}^* \end{pmatrix} \begin{pmatrix} \mathcal{X}^\nu \\ \mathcal{Y}^\nu \end{pmatrix} = \omega_\nu \begin{pmatrix} \mathcal{X}^\nu \\ \mathcal{Y}^\nu \end{pmatrix}, \quad (8)$$

where

$$\mathcal{A} = \begin{pmatrix} A_{11'} & A_{12} \\ A_{21} & A_{22'} \end{pmatrix}, \quad \mathcal{B} = \begin{pmatrix} B_{11'} & B_{12} \\ B_{21} & 0 \end{pmatrix}, \quad (9)$$

$$\mathcal{X}^\nu = \begin{pmatrix} X_1^\nu \\ X_2^\nu \end{pmatrix}, \quad \mathcal{Y}^\nu = \begin{pmatrix} Y_1^\nu \\ Y_2^\nu \end{pmatrix}. \quad (10)$$

The indices 1 and 2 denote $1p1h$ and $2p2h$ configurations, respectively. Thus, the $11'$ block in the matrices \mathcal{A} and \mathcal{B} corresponds to the standard RPA A and B matrices. The 12 and 21 blocks contain the $1p1h - 2p2h$ coupling, and the $22'$ block (the B part of which vanishes) contains the $2p2h$ part of the matrix.

It is straightforward to show that the SRPA equations may be written as RPA-like equations with energy-dependent RPA matrices $A_{11'}(\omega)$ and $B_{11'}(\omega)$,

$$\begin{aligned}
A_{11'}(\omega) &= A_{11'} + \sum_{2,2'} A_{12}(\omega + i\eta - A_{22'})^{-1} A_{2'1'} - \sum_{2,2'} B_{12}(\omega + i\eta + A_{22'})^{-1} B_{2'1'}, \\
B_{11'}(\omega) &= B_{11'} + \sum_{2,2'} A_{12}(\omega + i\eta - A_{22'})^{-1} B_{2'1'} - \sum_{2,2'} B_{12}(\omega + i\eta + A_{22'})^{-1} A_{2'1'}.
\end{aligned} \tag{11}$$

These are just the analogs of the ω -dependent interaction $V(\omega)$ from Sec. II in the more general particle-hole basis. Without so-called rearrangement terms, B_{12} and B_{21} would vanish, there would be no correction to $B_{11'}$, which would simply become the corresponding RPA matrix (no energy dependence) and the last term in Eq. (11) would be zero. We include rearrangement terms here, however.

Let us denote by $E_{11'}(\omega)$ and $F_{11'}(\omega)$ the energy-dependent corrections to $A_{11'}$, and $B_{11'}$:

$$\begin{aligned}
E_{11'}(\omega) &= \sum_{2,2'} A_{12}(\omega + i\eta - A_{22'})^{-1} A_{2'1'} - \sum_{2,2'} B_{12}(\omega + i\eta + A_{22'})^{-1} B_{2'1'}, \\
F_{11'}(\omega) &= \sum_{2,2'} A_{12}(\omega + i\eta - A_{22'})^{-1} B_{2'1'} - \sum_{2,2'} B_{12}(\omega + i\eta + A_{22'})^{-1} A_{2'1'}.
\end{aligned} \tag{12}$$

The subtraction procedure, in this matrix context, corrects the RPA-like matrices by subtracting from $A_{11'}(\omega)$ and $B_{11'}(\omega)$ the static parts $E_{11'}(0)$ and $F_{11'}(0)$, respectively (the analogs of U in Sec. II):

$$A_{11'}^S(\omega) = A_{11'}(\omega) - E_{11'}(0), \tag{13}$$

$$B_{11'}^S(\omega) = B_{11'}(\omega) - F_{11'}(0). \tag{14}$$

$A_{11'}^S(\omega)$ and $B_{11'}^S(\omega)$ are then substituted for $A_{11'}(\omega)$ and $B_{11'}(\omega)$ in the energy-dependent RPA-like equations. One can then return to energy-independent equations with larger matrices, obtaining

$$\begin{aligned}
\mathcal{A}_F^S &= \begin{pmatrix} A_{11'} + \sum_{2,2'} A_{12}(A_{22'})^{-1} A_{2'1'} + \sum_{2,2'} B_{12}(A_{22'})^{-1} B_{2'1'} & A_{12} \\ & A_{21} & A_{22'} \end{pmatrix}, \\
\mathcal{B}_F^S &= \begin{pmatrix} B_{11'} + \sum_{2,2'} A_{12}(A_{22'})^{-1} B_{2'1'} + \sum_{2,2'} B_{12}(A_{22'})^{-1} A_{2'1'} & B_{12} \\ & B_{21} & 0 \end{pmatrix}.
\end{aligned} \tag{15}$$

The subscript F stands for “full” here. We will contrast the full calculation later with a “diagonal approximation”. We note that the restoration of the RPA in the $\omega = 0$ limit implies that the static polarizability, related to the inverse energy-weighted moment m_{-1} , is the same in the subtracted SRPA as in the RPA. Because m_{-1} is generally larger in the standard SRPA than in the RPA, this fact already suggests that subtraction, which restores the RPA m_{-1} , must shift energy upwards with respect

to the ordinary SRPA.

The matrix $A_{22'}$ has to be inverted to construct the matrices in Eq. 15. If the energy cutoff is very large, the dimensions of the matrix become even more so and the inversion becomes computationally costly. We therefore will sometimes use a diagonal approximation in which off-diagonal terms of the matrix $A_{22'}$ are discarded only in the correction terms. The subtracted SRPA matrices, which we call \mathcal{A}_D^S and \mathcal{B}_D^S , then are

$$\begin{aligned}
\mathcal{A}_D^S &= \begin{pmatrix} A_{11'} + \sum_2 A_{12}(A_{22}^{diag})^{-1} A_{21'} + \sum_2 B_{12}(A_{22}^{diag})^{-1} B_{21'} & A_{12} \\ & A_{21} & A_{22'} \end{pmatrix}, \\
\mathcal{B}_D^S &= \begin{pmatrix} B_{11'} + \sum_2 A_{12}(A_{22}^{diag})^{-1} B_{21'} + \sum_2 B_{12}(A_{22}^{diag})^{-1} A_{21'} & B_{12} \\ & B_{21} & 0 \end{pmatrix}.
\end{aligned} \tag{16}$$

With this approximation the computational effort is con-

siderably reduced. When Eq. (16) is used, one can ei-

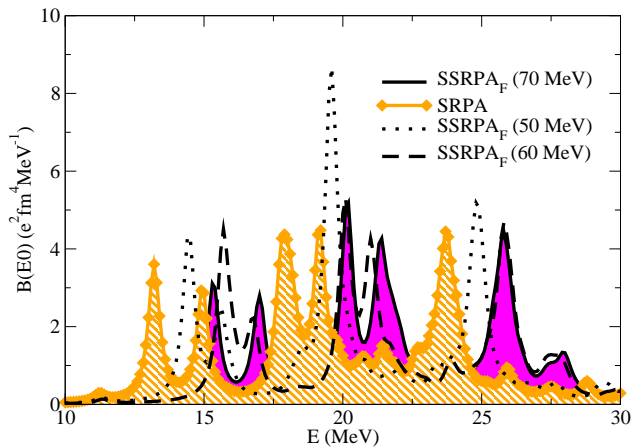


Figure 1. (Color online) Isoscalar monopole response for the nucleus ^{16}O , calculated in the standard SRPA (orange diamonds and orange area), and with the SSRPA_F , with a cutoff for the correction terms at 50 (black dotted line), 60 (black dashed line), and 70 (black solid line and magenta area) MeV.

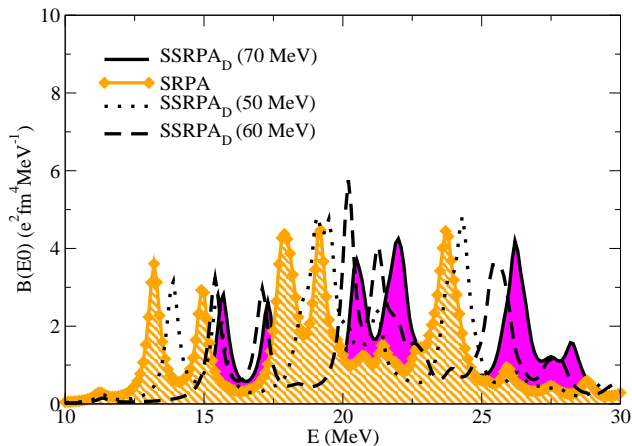


Figure 2. (Color online) Same as in Fig. 1, but in the diagonal approximation SSRPA_D .

ther keep only the unperturbed energies or include also the residual interaction in A_{22}^{diag} to compute the correction terms. We have verified that the two choices lead to very similar results. In what follows, we show the results obtained by neglecting the residual interaction.

IV. SUBTRACTED SPECTRA AND ACCURACY OF THE DIAGONAL APPROXIMATION

Let us first show the effect of the subtraction method on the SRPA results, for illustration in the isoscalar monopole and quadrupole channels of ^{16}O . We perform HF-RPA calculations with a cutoff on the $1p1h$ configurations at 100 MeV. For the $2p2h$ space in the SRPA calculations, we take the cutoff to be at 70 MeV and 50 MeV for the monopole and the quadrupole cases, respectively.

Those values lead to about 5000 $2p2h$ configurations in each of the two cases. This number is small enough so that we can still fully invert the matrix A_{22} , to perform the subtraction.

We use the acronyms SSRPA_F to denote the subtracted SRPA in the full scheme, Eq. (15), and SSRPA_D to denote the subtracted SRPA with the diagonal approximation in the correction terms, Eq. (16). In all the figures that follow, we fold the calculated response with a Lorentzian of width 0.5 MeV.

Fig. 1 shows the isoscalar monopole strength distribution, calculated with the unmodified SRPA and with the SSRPA_F , using a cutoff in the correction term equal to 50, 60, and 70 MeV. In the last of these cases, all the SRPA $2p2h$ configurations are included in the correction. The effect of the subtraction, as we expected, is to shift the SRPA spectrum upwards, by amounts that increase with the cutoff in the correction terms. The important differences between the three subtracted strength functions indicate that it is crucial to include all the $2p2h$ states in the correction terms containing $(A_{22'})^{-1}$ in Eq. (15). The calculation must be coherent, that is, the $2p2h$ spaces used in the original SRPA matrices and in the correction terms should be the same.

Fig. 2 shows the same results with the diagonal approximation SSRPA_D and Fig. 3 compares the full and diagonal subtracted SRPA results with the 70-MeV cutoff in the correction terms. We observe that the SSRPA_F and SSRPA_D results are very similar, the difference being a small systematic shift to larger excitation energies in the SSRPA_D .

Figs. 4, 5, and 6 display the same results as Figs. 1, 2, and 3, respectively, but in the isoscalar quadrupole channel (where the $2p2h$ cutoff is at 50 MeV in the SRPA calculation). The cutoffs in the correction terms are at

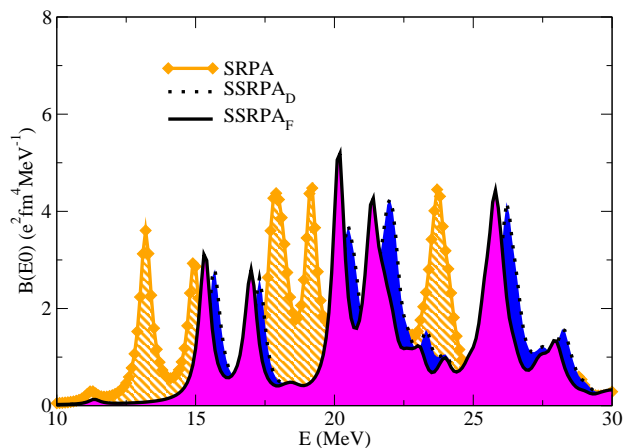


Figure 3. (Color online) Isoscalar monopole response for the nucleus ^{16}O , calculated in the SRPA without subtraction (orange diamonds and orange area), in the SSRPA_F (black solid line and magenta area) and in the SSRPA_D (black dotted line and blue area), with a cutoff in the correction terms at 70 MeV.

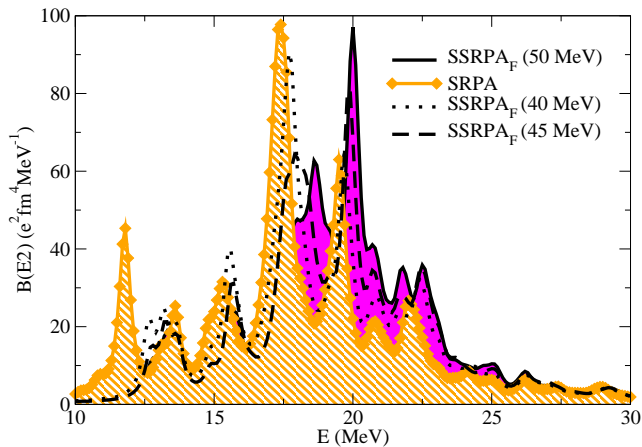


Figure 4. (Color online) Same as in Fig. 1 but for the isoscalar quadrupole response. The $2p2h$ cutoffs in the correction terms are now at 40, 45, and 50 MeV.

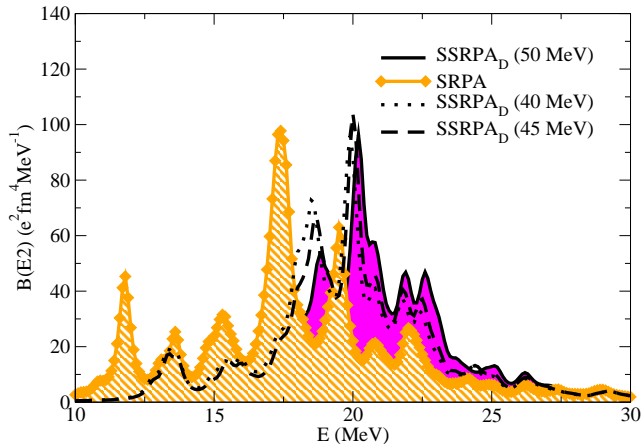


Figure 5. (Color online) Same as in Fig. 2 but for the isoscalar quadrupole response.

40, 45, and 50 MeV. The remarks made about the first three figures apply here as well. In Fig. 6, the same systematic shift between the results of the full and diagonal subtracted calculations is visible.

To better understand the extra shift produced by the $SSRPA_D$, we plot in Figs. 7 and 8 the diagonal part of the correction in the monopole and quadrupole channels, respectively, calculated for each $1p1h$ state with the $SSRPA_F$ and $SSRPA_D$, with the largest cutoff in each multipole. The correction introduced by the subtraction modifies the diagonal part of the RPA A matrix, and induces a shift in the $1p1h$ unperturbed excitation energies. The figures show that the diagonal correction term is always larger in the $SSRPA_D$ than in the $SSRPA_F$. This leads to the extra shift of the spectrum found in the $SSRPA_D$. The difference, while systematic, is small. The result suggests that the dominant effect of the correction comes from its diagonal part, which modifies the unperturbed excitation energies.

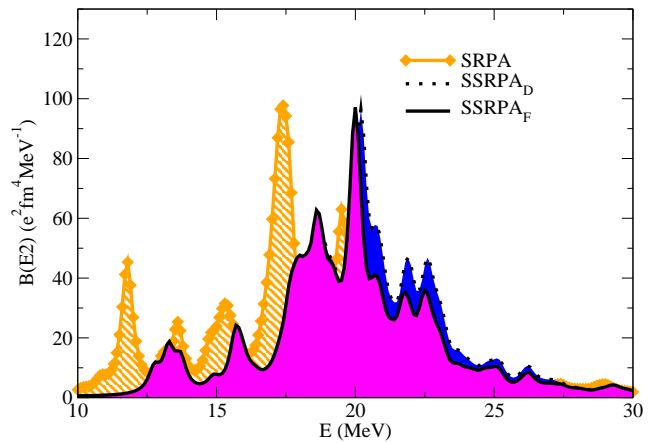


Figure 6. (Color online) Same as in Fig. 3 but for the isoscalar quadrupole response. The $2p2h$ cutoff for the correction terms is at 50 MeV.

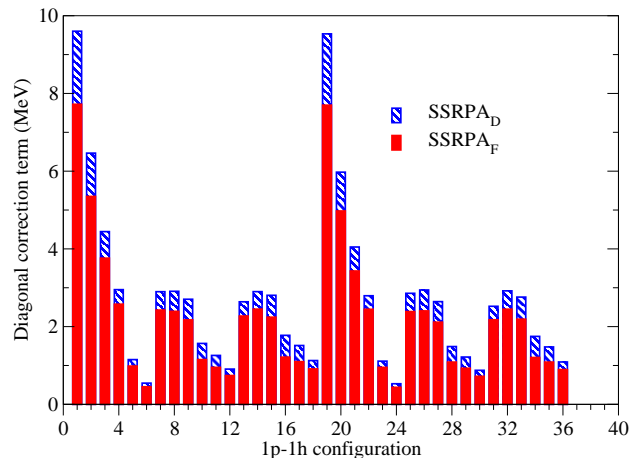


Figure 7. (Color online) Diagonal part of correction term for each $1p1h$ configuration that contributes to the monopole strength, for the $SSRPA_F$ (red full bars) and the $SSRPA_D$ (blue dashed bars), with a cutoff at 70 MeV in the correction terms.

We turn now to low-lying excited states. Fig. 9 shows the first 0^+ and 2^+ states obtained in the unmodified SRPA and in the $SSRPA_F$ and $SSRPA_D$, with different $2p2h$ cutoffs in the correction terms. Only states with a $B(E0)$ or $B(E2)$ larger than $10^{-2} e^2 fm^4$ are shown. Interestingly, the effect of the correction is now different than what we found for the giant resonances. Low-lying states are not strongly modified by the subtraction method. This suggests that these states have a dominant multiparticle–multi-hole nature, as a close examination of the \mathcal{X} 's and \mathcal{Y} 's from Eq. (10) verifies. They cannot be affected by the subtraction because it acts only on the $1p1h$ sector of the SRPA matrix.

Before comparing our results with those obtained in the RPA and with the experimental values, we analyze the robustness of the subtracted SRPA model. We focus on the 0^+ channel. We initially carry out standard SRPA

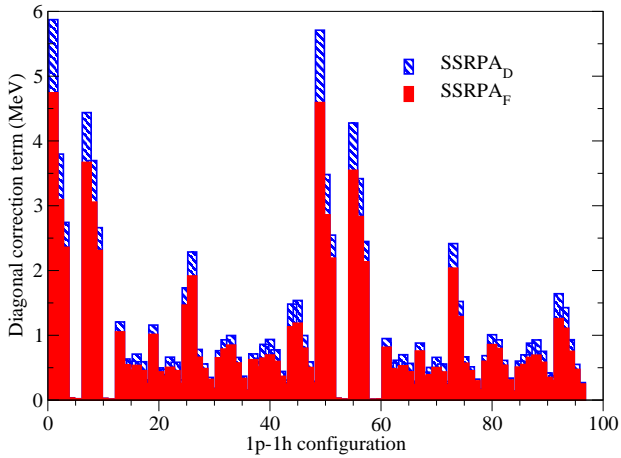


Figure 8. (Color online) Same as in Fig. 7, but for the quadrupole channel, with a cutoff at 50 MeV in the correction terms.

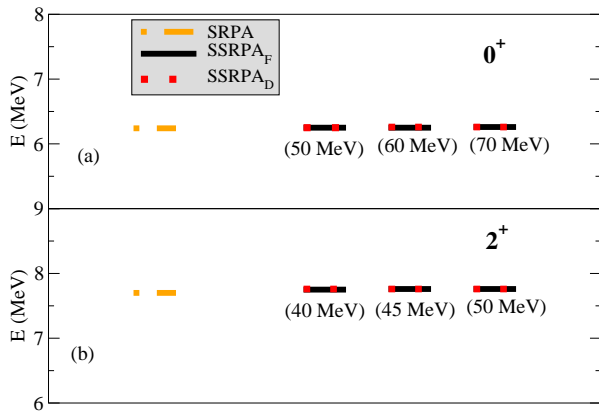


Figure 9. (Color online) First 0^+ (a) and 2^+ (b) states calculated with the standard SRPA, the SSRPA_F , and the SSRPA_D , with different cutoffs in the correction terms (in parentheses).

calculations with several cutoffs up to 90 MeV on the $2p2h$ configurations, finding, as expected, that the shift to lower energies (with respect to the RPA spectrum) becomes more and more pronounced as the cutoff energy increases [5]. The number of $2p2h$ configurations is too large in these high-cutoff SRPA calculations to invert the matrix $A_{22'}$, and so when examining the subtraction correction we use the diagonal approximation. Fig. 10 shows the resulting isoscalar monopole responses, with cutoffs for the correction terms at 70, 80, and 90 MeV. In each case, this cutoff is the same as that in the corresponding unsubtracted SRPA calculation. The three strength functions are very similar. The same is true of the low-lying 0^+ state. Its energy with the 70, 80, and 90 MeV cutoff is 6.26 MeV, 6.13 MeV, and 5.96 MeV, respectively. The difference between the highest and lowest of these numbers is only 5%. We can conclude that the subtraction procedure not only rectifies the SRPA energy

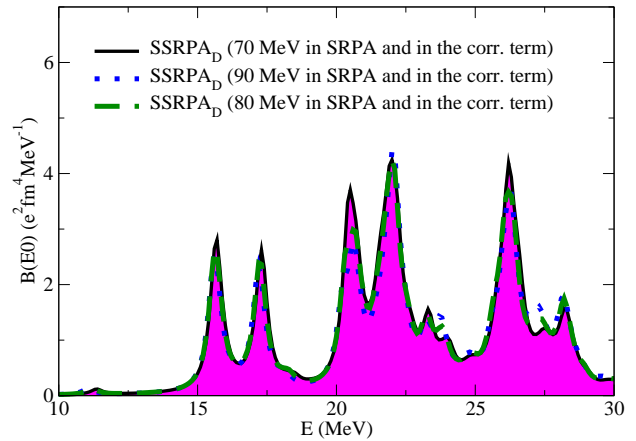


Figure 10. (Color online) Isoscalar monopole response in the diagonal approximation with cutoff for the correction terms at 70 (black line and magenta area), 80 (green dashed line), and 90 (blue dotted line) MeV.

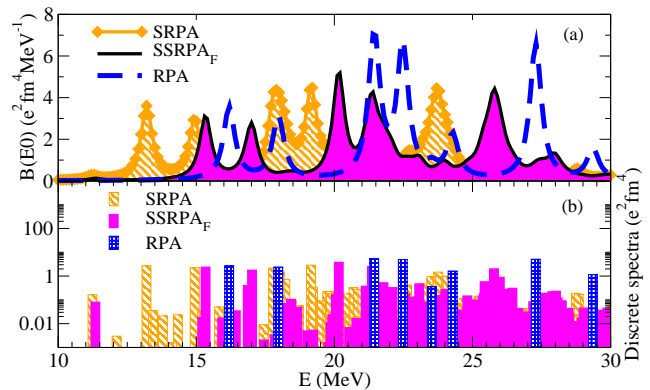


Figure 11. (Color online) (a): Isoscalar monopole response in the standard SRPA (orange diamonds and orange area), RPA (blue dashed line), and the SSRPA_F (black solid line and magenta area); (b): Discrete spectra (binned strength) obtained with the SRPA (orange dashed bars), the RPA (blue dotted bars) and the SSRPA_F (magenta solid bars).

shifts for giant resonances, but also provides much more robust (cutoff-insensitive) predictions for both giant resonances and low-lying states.

V. COMPARISON WITH RPA AND EXPERIMENT

We turn finally to the quality of the subtracted SRPA results in comparison with those of the ordinary RPA and with experiment. We again restrict ourselves to the monopole and quadrupole cases. For these comparisons, we carry out fully the subtraction, with the maximal cutoffs given earlier (50 and 70 MeV for the monopole and quadrupole channels, respectively).

The top panels of Figs. 11 and 12, respectively, compare the monopole and quadrupole strength distributions

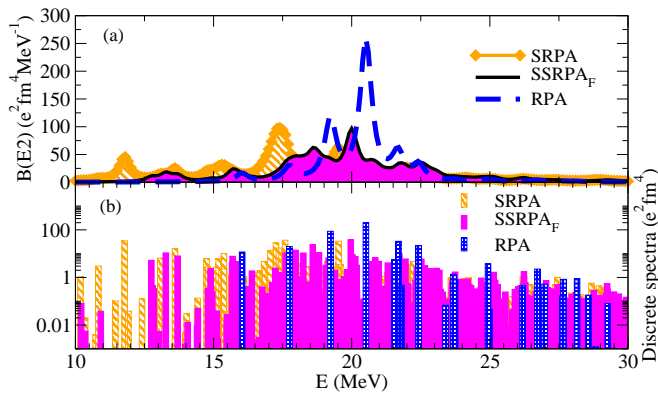


Figure 12. (Color online) Same as in Fig. 11 but for the quadrupole strength.

of the ordinary SRPA, the SSRPA_F , and the RPA. We observe that the strong shift that the ordinary SRPA provides with respect to the RPA is significantly reduced by the subtraction procedure. The lower panels of the same figures display the discrete (binned) strengths. The fragmentation and the width of the excitation are provided by both SRPA models (with and without subtraction). They are described in a natural way by the extremely dense discrete $2p2h$ configurations obtained in both cases. The subtraction procedure does not affect this feature but only shifts states to higher energies. The ordinary RPA, by contrast, produces a scattered set of states without any fragmentation.

Before comparing with experiment, we analyze the moments m_{-1} , m_0 , and m_1 of the strength–distribution, for the isoscalar quadrupole case, as an illustration. In Fig. 13 we show the ratios of these moments, calculated in the SRPA, the SSRPA_F , and the SSRPA_D , to those of the RPA. We have varied the cutoff energy in the correction terms for the subtracted calculations. One observes first that m_0 and m_1 are the same in the RPA and in the SRPA, as expected. The corresponding subtracted–SRPA moments are different, however. The upward shift from subtraction means that m_1 must be larger with subtraction than without and m_{-1} , as noted earlier, must be smaller; the figure bears these conclusions out. Unsurprisingly, in addition, the full subtraction produces (at maximal cutoff) values that are closer to the RPA than does the diagonal approximation. The inverse moment m_{-1} is exactly the same in the SSRPA_F with maximal cutoff and in the RPA, as it must be (see Sec. III). The equality holds only when the calculation is fully coherent (full inversion and same $2p2h$ space in the matrices and in the correction term).

Finally, we compare our results with experiment. Figs. 14 and 15 compare the RPA and subtracted SRPA spectra with experimental strength distributions [33]. We have extracted the experimental fractions of the EWSR from the top and the bottom panels of Fig. 6 in Ref. [33]. To compare with our results we have multiplied our fractions of the monopole EWSR by 0.48 and the

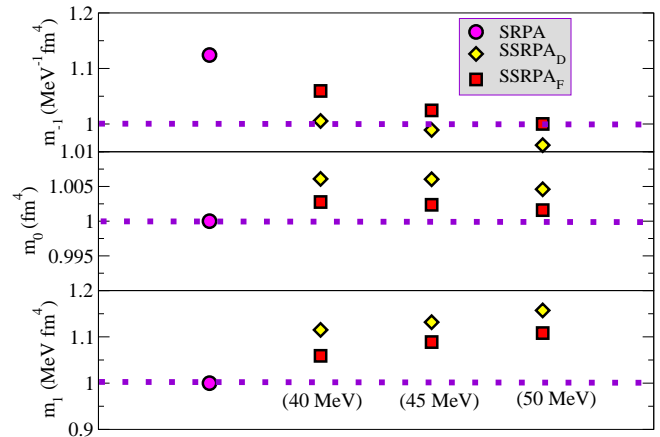


Figure 13. (Color online) Ratios of the moments m_{-1} , m_0 , and m_1 of the quadrupole strength distribution in the SRPA (purple circles), the SSRPA_F (red squares), and the SSRPA_D (yellow diamonds) to those in the RPA for increasingly high cutoffs in the correction terms, at 40, 45, and 50 MeV.

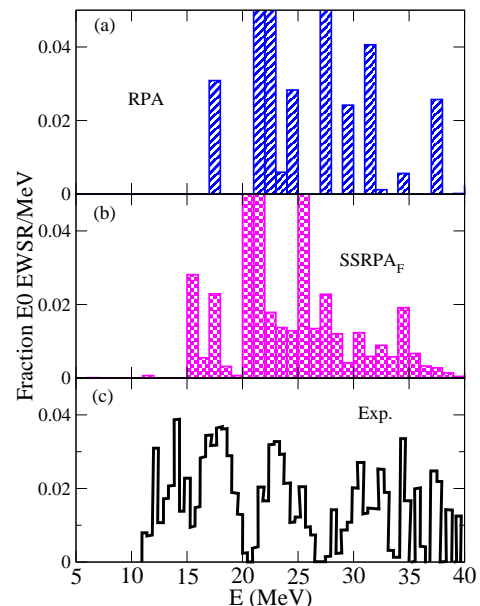


Figure 14. (Color online) Fraction of the $E0$ EWSR in the RPA (a) and in the SSRPA_F (b). The experimental fraction, from Ref. [33] is in panel (c).

quadrupole EWSR by 0.53. The reason is that only the 48% of the $E0$ EWSR and the 53% of the $E2$ EWSR have been measured [33]. Note that the scales of the vertical axes in panels (a) and (b) are chosen equal to those of the corresponding panels (c) for an easier comparison.

We observe that, for the monopole case, the RPA produces a strength distribution that is higher in energy than experiment by several MeV. This feature of the RPA for the nucleus ^{16}O is well known. In Ref. [33], for example, the RPA results of Ref. [34] were shifted downwards by 4.2 MeV to agree with the measured centroid. The SRPA

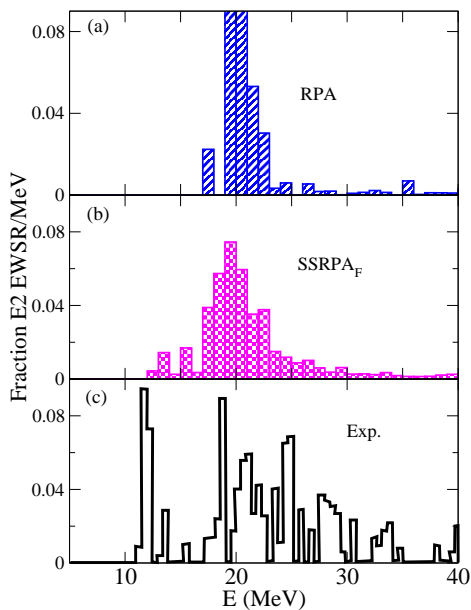


Figure 15. (Color online) Same as in Fig. 14 but for the E2 EWSR.

results produced here (without subtraction) would be in much better agreement with experiment because there is much more strength at low energies, and in particular there is non-negligible strength between 10 and 15 MeV (see Fig. 11). One should keep in mind, however, that the SRPA results without subtraction are strongly cutoff dependent; strength would be shifted to even lower energies if the cutoff energy were increased significantly, worsening the agreement with experiment. In contrast, as shown in this work, the results obtained with the subtraction procedure are quite stable against variations in the cutoff. Though the subtracted SRPA produces a reduced downward shift from the RPA than the ordinary SRPA with the cutoff chosen here (and as a result appears to agree less well with experiment) the shift is nevertheless in the right direction: Some strength appears between 10 and 15 MeV and there is much more strength between 15 and 20 MeV than in the RPA.

For the quadrupole case, the shift between the results of the RPA and those of the subtracted SRPA is less pronounced. The main difference between the two response functions is in the fragmentation, which is obviously much better described within the subtracted SRPA. Some strength is found between 10 and 15 MeV, as in the experimental distribution, while in the RPA the strength starts at higher energy.

Let us now analyze the low-lying states. Fig. 16 compares the SRPA, $SSRPA_F$, and RPA energies with those from experiment [35] for the first 0^+ and 2^+ states. The

RPA values are too high in energy and the SRPA results (with or without subtraction) are in good agreement with experiment. As already noted, the subtraction does not modify the energies of such states because their most important configurations are $2p2h$.

VI. CONCLUSIONS

We have applied to the SRPA a subtraction procedure proposed by Tselyaev [15] some years ago to overcome problems related to double counting in certain beyond-mean-field calculations. Ref. [22] showed that the subtraction method in extended RPA models, such as the SRPA, leads to stable solutions (the Thouless theorem may be extended and the stability condition satisfied).

We have presented applications to the nucleus ^{16}O with the Skyrme interaction SGII. We have verified that the subtracted SRPA provides very robust predictions, which are stable and very weakly cutoff dependent. Furthermore, the fulfillment of the stability condition, together with the elimination of double counting, substantially reduces the large anomalous shift downwards that the ordinary SRPA systematically produces with respect to the RPA strength.

This implementation of the SRPA model opens the door to numerous applications to reliably assess the effects of multiparticle-multipole configurations on the excitation of medium-mass and heavy nuclei.

ACKNOWLEDGMENTS

M.G. acknowledges the support of the International Associated Laboratory COLL-AGAIN.

J.E. acknowledges the support of the U.S. Department of Energy through Contract No. DE-FG02-97ER41019.

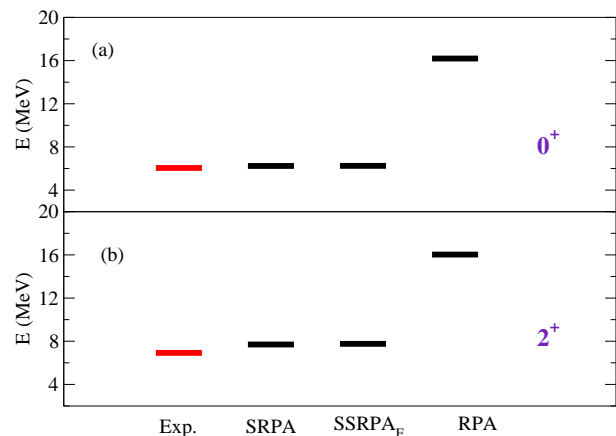


Figure 16. Comparison of values from the standard SRPA, the $SSRPA_F$, the RPA, and experiment for the energy of the first low-lying 0^+ (a) and 2^+ (b) states.

-
- [1] J. da Providencia, Nucl. Phys. 61, 87 (1965).
[2] C. Yannouleas, Phys. Rev. C 35, 1159 (1987).
[3] P. Papakonstantinou and R. Roth, Phys. Lett. B 671, 356 (2009).
[4] P. Papakonstantinou and R. Roth, Phys. Rev. C 81, 024317 (2010).
[5] D. Gambacurta, M. Grasso, and F. Catara, Phys. Rev. C 81, 054312 (2010).
[6] D. Gambacurta, M. Grasso, and F. Catara, J. Phys. G 38, 035103 (2011).
[7] D. Gambacurta, M. Grasso, and F. Catara, Phys. Rev. C 84, 034301 (2011).
[8] D. Gambacurta, M. Grasso, V. De Donno, G. Co, and F. Catara, Phys. Rev. C 86, 021304(R) (2012).
[9] T.H.R. Skyrme, Philos. Mag. 1, 1043 (1956).
[10] T.H.R. Skyrme, Nucl. Phys. 9, 615 (1959).
[11] D. Vautherin and D. Brink, Phys. Rev. C 5, 626 (1972).
[12] J. Dechargé and D. Gogny, Phys. Rev. C 21, 1568 (1980).
[13] J.F. Berger, M. Girod, D. Gogny, Comput. Phys. Commun. 63, 365 (1991).
[14] K. Moghrabi, M. Grasso, G. Colò, and N. V. Giai, Phys. Rev. Lett. 105, 262501 (2010).
[15] V.I. Tselyaev, Phys. Rev. C 75, 024306 (2007).
[16] E.V. Litvinova and V.I. Tselyaev, Phys. Rev. C 75, 054318 (2007).
[17] V. Tselyaev, *et al.*, Phys. Rev. C 79, 034309 (2009).
[18] A. Avdeenkov, S. Goriely, S. Kamenrdzhiev, and S. Krewald, Phys. Rev. C 83, 064316 (2011).
[19] E. Litvinova, P. Ring, and V. Tselyaev, Phys. Rev. C 75, 064308 (2007).
[20] E. Litvinova, P. Ring, and V. Tselyaev, Phys. Rev. C 78, 014312 (2008).
[21] E. Litvinova, P. Ring, and V. Tselyaev, Phys. Rev. Lett. 105, 022502 (2010).
[22] V.I. Tselyaev, Phys. Rev. C 88, 054301 (2013).
[23] D.J. Thouless, Nucl. Phys. 22, 305 (1961).
[24] P. Papakonstantinou, Phys. Rev. C 90, 024305 (2014).
[25] P. Ring and P. Shuck, *The Nuclear Many-Body Problem* (Springer-Verlag, Berlin, 1980).
[26] D. Gambacurta and F. Catara, Phys. Rev. B 81, 085418 (2010).
[27] N.V. Giai, and H. Sagawa, Phys. Lett. B 106, 379 (1981); Nucl. Phys. A 371, 1 (1981).
[28] see, e.g., *A Primer in Density Functional Theory*, C. Fiolhais F. Nogueira, and M. Marques, eds., Springer (1997).
[29] P. Hohenberg and W. Kohn, Phys. Rev. 136, 8864 (1964).
[30] W. Kohn and L.J. Sham, Phys. Rev. 140, A1133 (1965).
[31] J. Engel, Phys. Rev. C 75 014306 (2007).
[32] E. Runge and E.K.U. Gross, Phys. Rev. Lett. 52, 997 (1984).
[33] Y.-W. Lui, H.L. Clark, and D.H. Youngblood, Phys. Rev. C 64, 064308 (2001).
[34] Z. Ma, N. Van Giai, H. Toki, and M. L’Huillier, Phys. Rev. C 55, 2385 (1997).
[35] F. Ajzenberg-Selove, Nucl. Phys. A 375, 1 (1985).